Eur. Phys. J. AP **15**, 199–206 (2001)

The European Physical Journal
Applied Physics
© EDP Sciences 2001

Loss of plasma scaling with magnetic field, pressure and discharge current in a CUSP confined plasma

A. Anukaliani and V. Selvarajan[a]

Department of Physics, Bharathiar University, Coimbatore, 641046, India

Received: 8 April 1999 / Revised: 22 January 2001 / Accepted: 12 March 2001

Abstract. The confinement properties of a low beta argon discharge plasma in a spindle cusp magnetic field was investigated. Plasma was produced by ionisation collisions by the electrons which were produced by thermionic emission of electrons. The central problem involved with plasma confinement by a cusped magnetic field is the loss of particles along the flux lines. Electron and ion leak widths were studied in the ring and point cusps and measured over a range of magnetic field strengths (B), neutral pressures (P) and discharge currents (I_{d}). It was found that the leak width was reduced with increase in I_{d} and B. The ion leak widths were found to be larger than the electron leak widths. The normalised effect of magnetic field and pressure on ion and electron leak widths in cusps are reported, compared and discussed. The dependence of electron and ion leak widths on plasma densities were also studied. At very low pressures, high plasma densities and high magnetic field strengths, a quasineutrality condition was attained.

PACS. 52.55. Lf Field-reversed configurations, rotamaks, astrons, ion rings, magnetized target fusion, and cusps

1 Introduction

Cusped magnetic fields are widely used in laboratory devices due to their ability to confine large volume uniform quiescent plasmas. Magnetic cusps are being investigated for use in ion beam sources, plasma etching reactors, ion implantation, plasma nitriding, etc. Kitsunezaki *et al.* [1], Hershkowitz *et al.* [2] and Leung *et al.* [3] have reported that the leakage half width scaled with the hybrid larmor radius $(r_{\mathrm{i}}r_{\mathrm{e}})^{1/2}$ where r_{i} and r_{e} are the ion and electron larmor radii respectively. Haines [4] discussed their experiments and held the ion acoustic instabilities and visco resistive sheaths as possible explanation for the hybrid leak widths. Hershkowitz *et al.* [5] and Fujita *et al.* [6] have reported hybrid leak widths in a low beta plasma confined by a permanent magnetic cusp. Kozima *et al.* [7] have studied plasma instabilities excited around a line cusp magnetic field and have also reported hybrid leak widths. However leak widths of the order of ion larmor radius in a laser produced high beta plasmas were reported by Kogoshi *et al.* [8] and Pechacek *et al.* [9]. A theoretical attempt was made by Knorr *et al.* [10] to calculate the width of an escaping plasma in a picket fence and they reported hybrid leak widths. Knorr *et al.* [11] derived an expression for cusp leak width by considering the electric field (originating from the charge separation) and showed that the effect of scattering of ions from the cusp region by fast electrons is important for the diffusion across the magnetic field. In 1986 Bosch and Merlino [12] experimented on ring and point cusp leak widths and made a model in which they derived a cusp loss width that satisfied their experimentally obtained scaling loss. Mukherjee *et al.* [13] produced a plasma by electron impact ionisation of nitrogen based gas mixtures and measured its densities by confining it in a single cusp magnetic field for the surface treatment of metals (plasma nitriding). In 1998 Morishita *et al.* [14] estimated the cusp leak width of Jaeri's Kamboko source (multi cusp negative ion source) and obtained a width of about ten times the value evaluated by two times ion larmor radius on the surface of cusp magnet.

In all the above applications the plasma leak is very important since it governs the power and particle balance of the confined plasma. The efficiency of cusp devices for plasma confinement (surface treatment of metals) depends on plasma losses from cusps. The present report is based on the study of the production and confinement of plasma using a cusped magnetic field configuration. Of particular interest are the profiles of plasma escaping through the flux lines, characterized by their full width at half maximum (FWHM) called the cusp leak width. The dependence of electron and ion leak widths (in the ring and point cusps) of the confined system was measured over a range of magnetic fields, discharge currents and neutral pressures.

2 Experimental details

The experimental apparatus consisted primarily of four systems:

(1) Plasma generation system;

[a] e-mail: physics@as250.bharathi.ernet.in

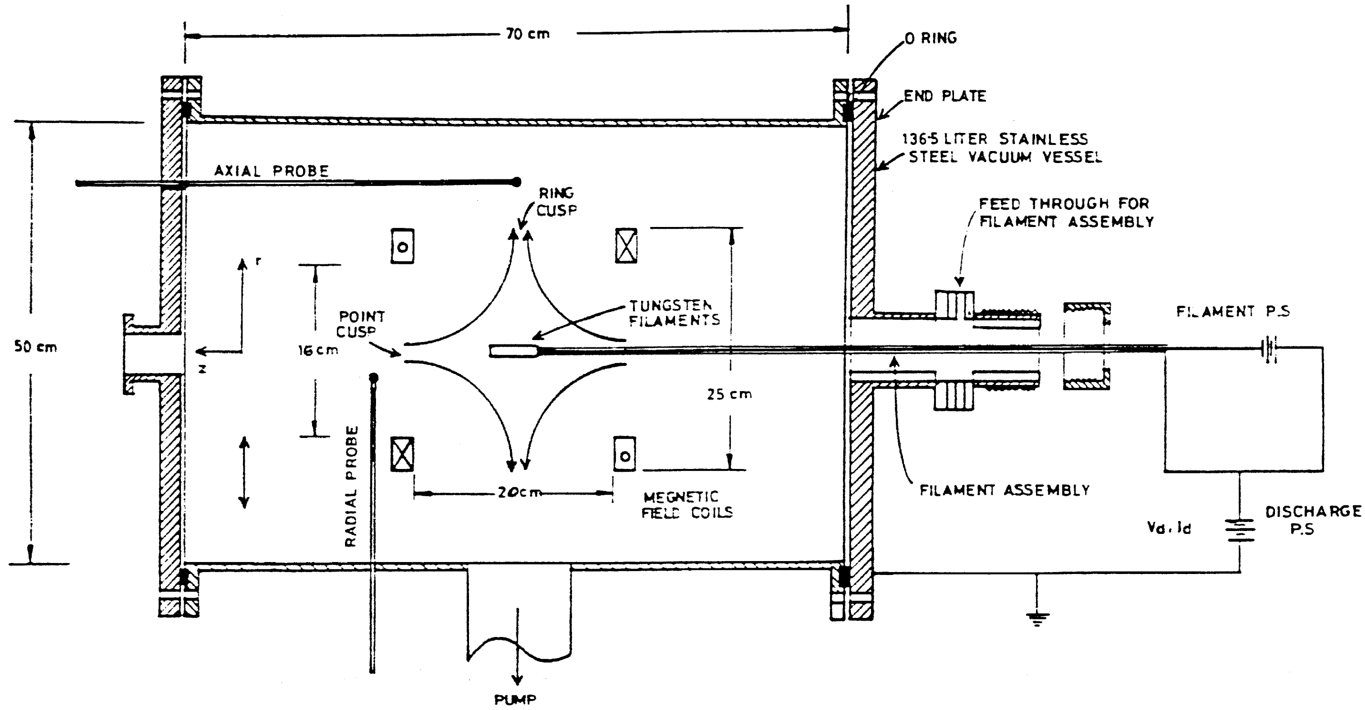

Fig. 1. Schematic diagram of plasma chamber.

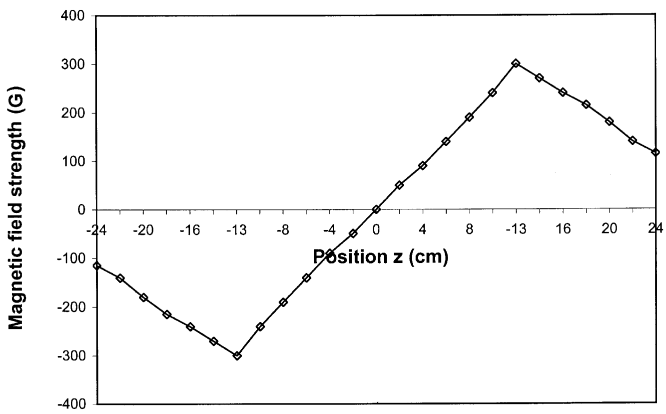

Fig. 2. Magnetic field strength *versus* position on the z axis with the maximum current of 250 A passing through the coils.

(2) vacuum system;
(3) magnetic field system;
(4) diagnostics.

The plasma chamber is presented schematically in Figure 1. It consists of a cylindrical vacuum chamber (water cooled) made of SS 304, 5 mm thick, 700 mm in length and 500 mm in diameter. The chamber has ports for feed throughs and viewing. The chamber was pumped down to a pressure of 2×10^{-5} mb and was filled with argon. Argon pressure was then reduced to the required operating pressures. The pressures were measured using pirani and penning gauges. The chamber was water cooled through tubes on its lateral surface.

A filament assembly was used for thermionic emission of electrons. Tungsten filaments of 0.05 cm dia and 7 cm length were mounted between two copper discs. The filament current was passed through a copper rod to one of the discs from which it returned coaxially through the filaments, to the other disc and a copper tube. The system was also water cooled.

An accelerating potential of 70 to 80 V was applied between the filaments and the walls of the chamber. The filaments were made negative and the walls were grounded. A current of 14 A was passed through each filament and made to emit electrons thermionically. The electrons were accelerated which produced a plasma through ionisation of argon gas in the chamber.

Two water cooled coils are located inside the chamber, with their planes parallel to each other, separated by a distance of 20 cm and perpendicular to the symmetry axis. Each coil is made up of five layers of five turns each of 6 mm copper tubing enclosed in an insulating sleeve. Inner and outer diameters of the magnetic coils are 16 cm and 25 cm respectively. By passing currents ranging from 50 A to 250 A in opposite directions in the coils, the required spindle cusp magnetic fields were produced. At a current of 250 A, the maximum field in the centre of the ring cusp was 160 G while the maximum field in the centre of the point cusp was 300 G. The magnetic field configuration for the maximum current is shown in Figure 2.

The major diagnostic tool used in this investigation is a cylindrical Langmuir probe, a tungsten wire of 0.05 cm dia and 0.45 cm length. The probes are capable of linear movement using Wilson feed throughs.

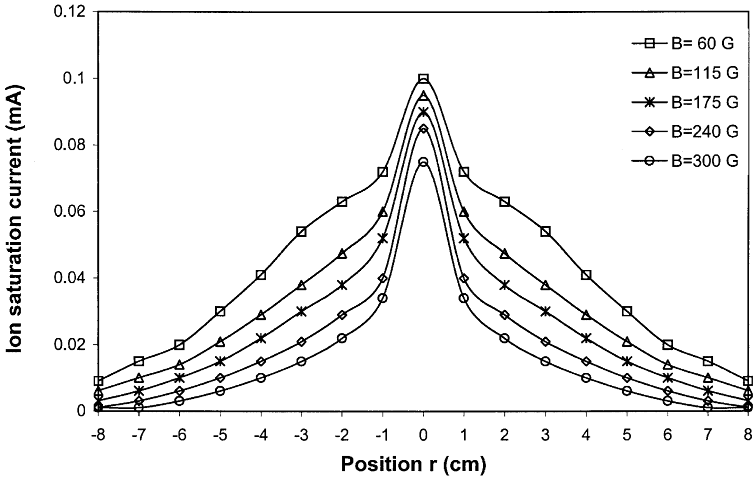

Fig. 3. Ion saturation current profile taken with a Langmuir probe across the point cusp ($z = 14$ cm, $P = 5 \times 10^{-4}$ mb, $I_d = 500$ mA).

3 Methodology

Initially, air was pumped down to 10^{-5} mb and the chamber was flushed with argon gas two to three times. Argon was filled to the required operating pressure and plasma was produced through collision of thermionically emitted electrons with argon atoms.

Langmuir probes were introduced into the chamber at the ring and point cusps using Wilson feed throughs. A bipolar power supply was used to bias the probe. The I-V characteristics of the probe were studied by keeping the probes at different radial and axial positions. Using the data on the linear portion (in the electron retardation region) of the characteristics the ln I_e (electron current) *vs.* V_p (probe potential) were plotted and the electron temperature of the plasma was calculated.

Electron temperature and plasma density were in the range of 3 to 4.5 eV and 10^{10} to 10^{12} cm^{-3} respectively.

The probe was kept at different locations across the point cusp with its length perpendicular to the symmetry axis. At each point, the maximum probe current (ion/electron) at the given pressure and magnetic field was measured. The current is a measure of the charge density at the point. The probe current was plotted against the probe position. The experiment was repeated at different selected pressures, magnetic fields and discharge currents and across the ring cusp.

4 Results and discussion

The results are illustrated in Figures 3 to 8 and Tables 1 to 4.

4.1 Cusp leak width

The maximum ion current to the probe as a function of position of the probe across the point cusp is shown in Figure 3. The positive ion density is proportional to the ion saturation current to the probe. Therefore the profile in Figure 3 can be interpreted as plots of relative density versus radial position. On the symmetry axis the current is maximum and decreases symmetrically on either side of it. The width of the profile at half maximum, *i.e.* the Full Width at Half Maximum (FWHM), is called the leak width and characterises plasma losses through the point cusp.

4.2 Leak widths as a function of magnetic field

The ion current profile in the point cusp at different magnetic field strengths are illustrated in Figure 3. It is seen that higher the strength of the magnetic field lower is the probe current at all positions and the profiles (peaks) become narrower as the strength of the magnetic field increases. Thus an increase of applied magnetic field reduces the plasma diffusing along the field lines. The scaling of the point cusp leak width with magnetic field for different pressures is shown in Figure 4. The variation of leak width ranges from 6.4 cm at 60 G to 1.6 cm at 300 G at a pressure of 5×10^{-4} mb and a discharge current (I_d) of 500 mA.

Theoretically, the leak width in a cusp configuration could be given as [15]

$$d = \left(\frac{2\overline{D}R}{C_s}\right)^{1/2} \tag{1}$$

where
$\overline{D}$ is the effective diffusion coefficient.
R is the coil radius.
C_s is the ion acoustic speed.

In the above formula, it is assumed that plasma escapes from the cusps at the ion acoustic speed while diffusing across the magnetic field due to collisions. In general, the diffusion coefficient $\overline{D}$ will be determined by electron neutral particle collisions (classical diffusion) and non classical diffusion (Bohm diffusion) [15] and if we assume that

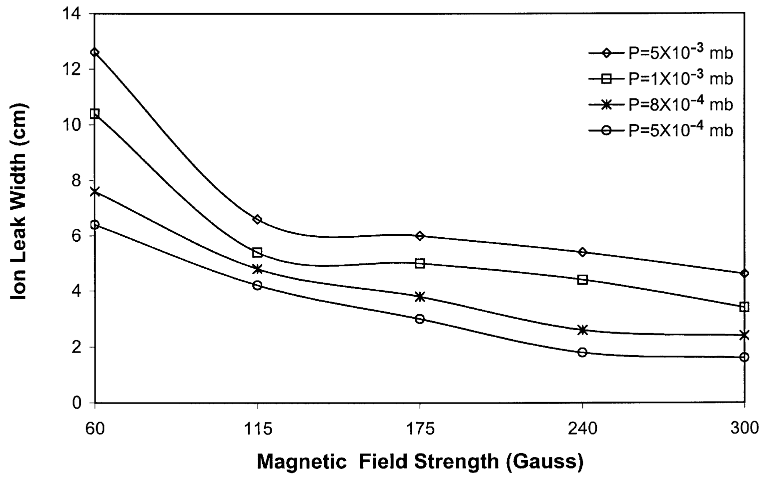

Fig. 4. Ion leak width in the point cusp *versus* B at four neutral pressures ($z = 14$ cm, $I_{\rm d} = 500$ mA).

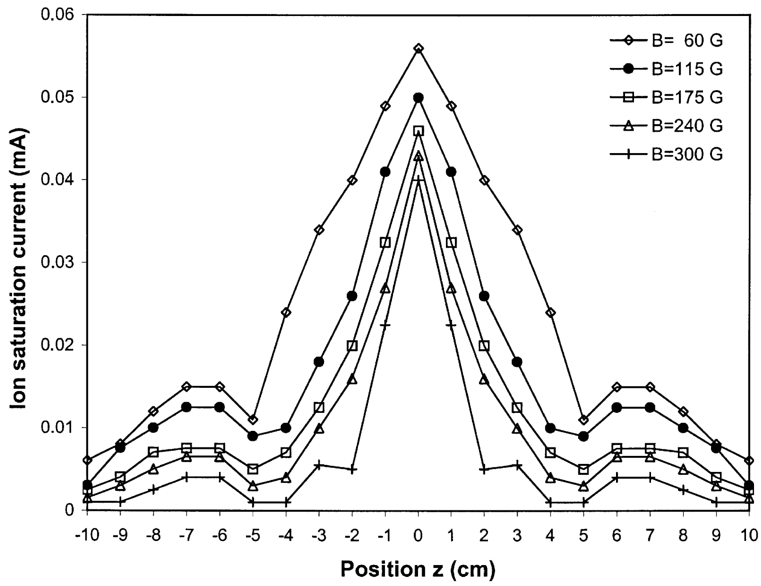

Fig. 5. Ion saturation current profile taken with a Langmuir probe across the ring cusp ($r = 19$ cm, $P = 5 \times 10^{-4}$ mb, $I_{\rm d} = 500$ mA).

these processes are linearly additive, we may write

$$\overline{D} = D_{\rm c} + D_{\rm B} \tag{2}$$

$$\overline{D} = \frac{r_{\rm ce}^2}{\tau_{\rm c}}\left(1 + \frac{T_{\rm i}}{T_{\rm e}}\right) + \frac{ckT_{\rm e}}{eB} \tag{3}$$

where $D_{\rm c}$ and $D_{\rm B}$ are the classical and Bohm diffusion coefficients and $\tau_{\rm c}$ is the electron neutral collisional relaxation time.

The probe current profiles of ions in the ring cusp region (at $P = 5 \times 10^{-4}$ mb) and the corresponding leak width variation as a function of magnetic field and for different pressures are shown in Figures 5 and 6 respectively. From the profile of Figure 5, it is seen that leakage profiles tended to have shoulders *i.e.*, regions in which the density remained nearly constant or increased slightly as the probe was moved from the centre of the cusp. Typically the ring cusp ion leak width varies from 7.2 cm at 40 G to 2.6 cm at 160 G ($P = 5 \times 10^{-4}$ mb and $I_{\rm d} = 500$ mA) and the variation is approximately linear beyond $B = 70$ G (Fig. 6) for all the pressures studied. The variation of ion and electron leak widths in the ring and point cusps for different discharge currents at $P = 5 \times 10^{-4}$ mb is given in Table 1.

The normalised reduction in leak width (reduction per unit increase of magnetic field) in the point cusp ($B = 60$ to 300 G) and ring cusp ($B = 40$ to 160 G) for $I_{\rm d} = 500$ mA, are given in Table 2. The normalised reduction in leak width with increase in B is faster at the ring cusp than at the point cusp. The results for electrons are qualitatively similar to those of ions. The normalised reduction in leak width at ring and point cusps for the same range of magnetic field ($B = 60$ to 160 G) are shown in Figures 7a and 7b.

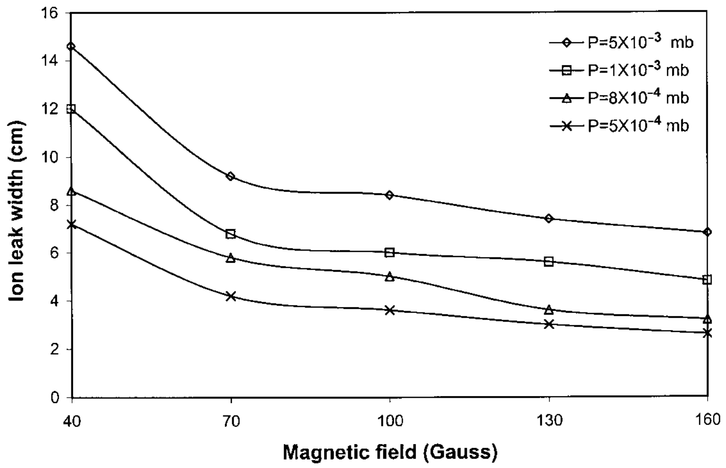

Fig. 6. Ion leak width in the ring cusp *versus* B at four neutral pressures ($r = 19$ cm, $I_d = 500$ mA).

Table 1. Variation of electron and ion leak widths with I_d in the ring and point cusps ($P = 5 \times 10^{-4}$ mb).

Discharge current I_d (mA)	Point cusp leak width (cm)									
	Ions					Electrons				
B (Gauss)→	60	115	175	240	300	60	115	175	240	300
200	8.2	5.8	4.6	3.4	3.0	5.4	3.4	2.2	1.4	1.2
350	7.2	4.8	3.8	2.4	2.2	5.8	3.4	2.6	1.6	1.4
500	6.4	4.2	3.0	1.8	1.6	6.2	3.8	2.6	1.8	1.6
	Ring cusp leak width (cm)									
	Ions					Electrons				
B (Gauss)→	40	70	100	130	160	40	70	100	130	160
200	9.0	6.0	5.4	4.4	4.0	4.0	2.8	2.4	1.4	1.2
350	7.8	5.4	4.8	3.4	3.0	4.8	3.6	2.8	1.8	1.6
500	7.2	4.2	3.6	3.0	2.6	5.6	4.0	3.4	2.4	2.0

Table 2. Reduction in leak width (normalised) $I_d = 500$ mA.

P (mb)	Point cusp leak width		Ring cusp leak width	
	$B = 60{-}300$ G		$B = 40{-}160$ G	
	Ions (%)	Electrons (%)	Ions (%)	Electrons (%)
5×10^{-4}	0.020	0.026	0.038	0.030
8×10^{-4}	0.022	0.024	0.045	0.035
1×10^{-3}	0.029	0.020	0.060	0.043
5×10^{-3}	0.033	0.019	0.065	0.047

4.3 Leak widths as a function of pressure

The scaling of the ion leak width in the ring cusp with pressure for different magnetic field strengths is shown in Figure 8. It is seen that at the neutral pressure of 5×10^{-4} mb ($I_d = 500$ mA) the ion leak width is 7.2 cm for 40 G and 2.6 cm for 160 G and as the pressure is increased to 5×10^{-3} mb, the ion leak width increases to 14.6 cm for 40 G and to 6.8 cm for 160 G. The increase in leak width with pressure is due to the diffusion caused by plasma neutral collisions. For a discharge current of 500 mA, the increase in leak width for ions at ring cusp, when the pressure is increased from 5×10^{-4} mb to 5×10^{-3} mb is 102.78% at $B = 40$ G and 161.54% at $B = 160$ G and at the point cusp it is 96.88% and 187.5% at $B = 60$ G and $B = 300$ G respectively.

The scaling of leak width with pressure and magnetic field can be explained using equation (1).

At low pressures, the plasma neutral collisions are rare. This suggests that the leak width is not determined by classical diffusion due to plasma neutral collisions. Here the Bohm diffusion [15] dominates and therefore

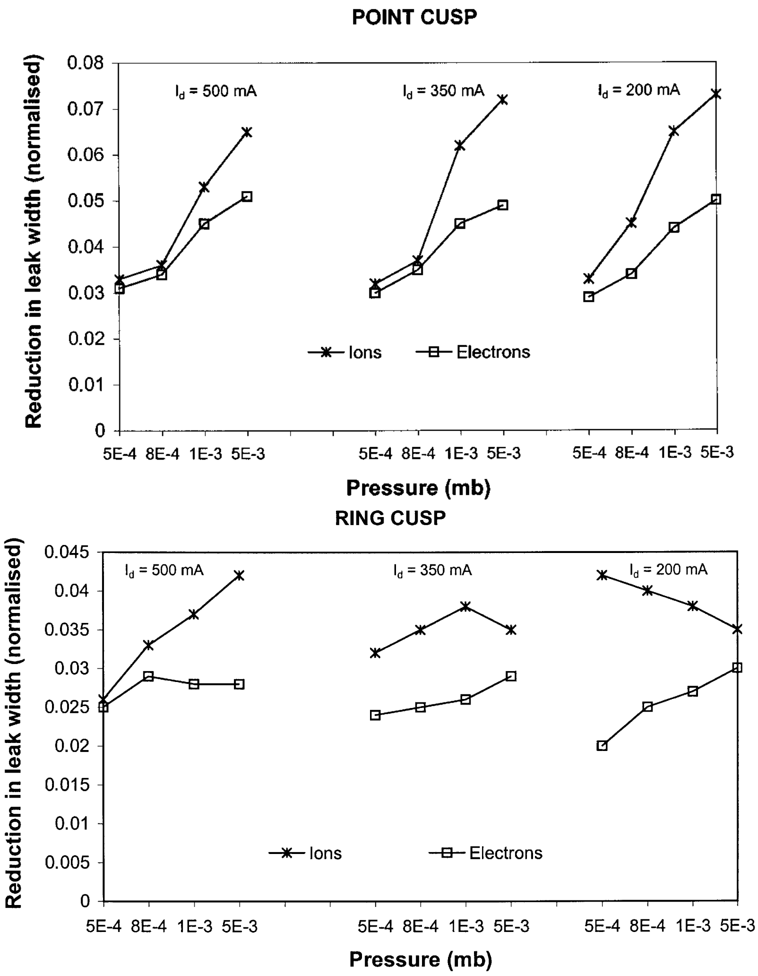

Fig. 7. Normalised reduction in leak width in the point and ring cusps for the same range of B (60–160 G).

equation (1) predicts a leak width given by:

$$d = \left[\frac{2R}{C_\mathrm{s}}\left(\frac{ck\,T_\mathrm{e}}{16eB}\right)\right]^{1/2} \quad \text{for } T_\mathrm{i} \ll T_\mathrm{e} \tag{4}$$

$$d \propto \left(\frac{m_\mathrm{i}^{1/4}T_\mathrm{e}^{1/4}}{\sqrt{B}}\right) \tag{5}$$

$$d \propto \left(\frac{1}{\sqrt{B}}\right)\cdot \tag{6}$$

Hence at low pressures and high magnetic fields the leak width does not depend on pressure but varies inversely as the square root of the magnetic field (Fig. 8). There is no change in leak width with increase in P at low P and high B values. In Table 3a, it is seen that at low pressures and high B values (240 and 300 G at point cusp and 130 and 160 G at ring cusp), the ratio of d values obtained experimentally is approximately equal to the reciprocal of the ratio of the square roots of the corresponding B values indicating good agreement with theory (Eq. (6)).

At sufficiently high pressures, plasma neutral collisions are important in the field free region and the plasma diffuses outward from the filaments. This suggests that the leak width is determined by neutral particle collisions at high pressures. Therefore equation (1) predicts a leak width given by [15]:

$$d = \left(\frac{2R}{C_\mathrm{s}}\left(\frac{r_\mathrm{ce}^2}{\tau_\mathrm{c}}\right)\left(1+\frac{T_\mathrm{i}}{T_\mathrm{e}}\right)\right)^{1/2} \quad \text{for } T_\mathrm{i} \ll T_\mathrm{e} \tag{7}$$

$$d \propto m_\mathrm{i}^{1/4}(\sigma T_\mathrm{e})^{1/2}\frac{\sqrt{P}}{B} \tag{8}$$

$$d \propto \frac{\sqrt{P}}{B} \tag{9}$$

where σ is the electron neutral collision cross section.

This suggests that for high neutral pressures, plasma neutral collisions are important in the field free region and the plasma diffused outward from the filaments.

At high P and low B values, for a given P the ratio of leak widths is equal to the inverse ratio of the magnetic fields (Eq. (9)). The experimental results are given in Table 3b. It is seen that for a given P value, the ratio of leak widths is in good agreement with inverse ratio of magnetic fields both at point and ring cusps.

For the point cusp, at sufficiently high pressures, (I_d = 200 mA and $P = 5\times10^{-3}$ mb) and low magnetic field

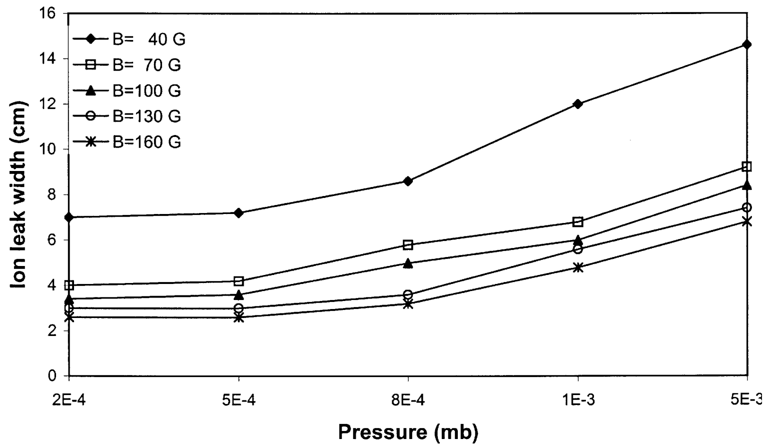

Fig. 8. Ion leak width in the ring cusp *versus* P for different values of B ($I_d = 500$ mA).

Table 3. (a) Comparison of ratio of leak widths obtained from theory and experiment Low P High B; (b) Comparison of ratio of leak widths obtained from theory and experiment High P Low B.

I_d (mA)	P (mb)	Low P High B			
		Point cusp ($\sqrt{B_2/B_1} = 1.2$) $B_1 = 240$ G and $B_2 = 300$ G		Ring cusp ($\sqrt{B_2/B_1} = 1.1$) $B_1 = 130$ G and $B_2 = 160$ G	
		Ions	Electrons	Ions	Electrons
200	5×10^{-4}	1.13	1.16	1.11	1.16
	8×10^{-4}	1.15	1.11	1.16	1.11
350	5×10^{-4}	1.09	1.14	1.13	1.13
	8×10^{-4}	1.13	1.09	1.15	1.18
500	5×10^{-4}	1.13	1.12	1.15	1.20
	8×10^{-4}	1.08	1.09	1.13	1.15

I_d (mA)	P (mb)	High P Low B			
		Point cusp ($B_2/B_1 = 1.92$) $B_1 = 60$ G and $B_2 = 115$ G		Ring cusp ($B_2/B_1 = 1.75$) $B_1 = 40$ G and $B_2 = 70$ G	
		Ions	Electrons	Ions	Electrons
200	5×10^{-3}	1.89	1.92	1.76	1.66
	8×10^{-3}	1.91	1.86	1.75	1.73
350	5×10^{-3}	1.94	1.85	1.76	1.67
	8×10^{-3}	1.90	1.83	1.79	1.78
500	5×10^{-3}	1.91	1.80	1.59	1.72
	8×10^{-4}	1.93	1.88	1.76	1.67

strengths ($B = 60$ G), the ion leak width (14.4 cm) is nearly as large as the coil inner diameter (16 cm) as in Table 1. For the same I_d, P and B at the ring cusp, the ion leak width (17.2 cm) is nearly as large as the coil inner separation (20.0 cm) and the escaping plasma is no longer constrained by the magnetic field but presumably by the mechanical constraint of the magnetic coils.

The leak width d has been calculated theoretically using equation (1) as a function of B ($I_d = 500$ mA). The experimental values of leak widths obtained for ions in the point and ring cusps and the theoretical values are illustrated in Table 4.

The experimental results are not in agreement with theory (Eq. (1)). At the point cusp the experimental and theoretical values of leak widths differ approximately by a factor of 3.5 and at ring cusp by a factor of 2 at low B and high P values. At high B and low P, the experimental and theoretical values differ by a factor of 3 both at the point cusp and the ring cusp.

The difference in the values of leak width obtained theoretically and experimentally is due to the approximations

Table 4. Experimentally and theoretically calculated values of ion leak widths at the point and ring cusps.

Low B High P ($I_d = 500$ mA, $P = 5 \times 10^{-3}$ mb)			
Point cusp ($B = 60$ G)		Ring cusp ($B = 40$ G)	
Theoretical	Experimental	Theoretical	Experimental
3.62	12.6	6.66	14.6
High B Low P ($I_d = 500$ mA, $P = 5 \times 10^{-4}$ mb)			
Point cusp ($B = 300$ G)		Ring cusp ($B = 160$ G)	
Theoretical	Experimental	Theoretical	Experimental
0.58	1.6	0.79	2.6

made in deriving the formula (Eq. (1)) for the leak width and the uncertainty in the numerical factor 1/16 in the Bohm diffusion coefficient [12]. Bosch and Merlino [12] on comparison found that the theoretical and their experimental values in general differed by a factor of three.

4.4 Leak width as a function of discharge current

The dependence of ring cusp electron and ion leak widths upon discharge currents (at $P = 5 \times 10^{-3}$ mb) is also shown in Table 1. The plasma density was varied by changing the filament current (which changes the discharge current) while all the other parameters were kept constant. It is seen that (at a pressure of 5×10^{-4} mb) as the discharge current (plasma density is proportional to discharge current) is increased from 200 mA to 500 mA, the ion and electron leak widths become comparable and the quasineutrality condition is satisfied. Also as the discharge current is increased the ion leak width decreases but the electron leak width increases. At relatively low discharge currents, ionisation will be small. Hence together with primary electrons, it is likely that plasma will be non neutral. Therefore the magnetic coil surfaces will acquire a negative potential and it will act as an accelerator for ions through the point and ring cusps. Also, the ion gyroradius will be much larger than the electron gyroradius. Hence, leak width for ions is larger than that for electrons at low discharge currents. As discharge current increases the plasma will become less and less nonneutral. The coil surfaces will acquire lesser negative potential thereby decreasing the acceleration on ions and increasing the flow of electrons. Hence, at one stage the leak width of ions and electrons will be comparable exhibiting quasineutrality. Bosch and Merlino [12] explained the difference in leak widths between ions and electrons at low and high plasma densities on the basis of self consistent electrostatic fields developed in the cusp region.

5 Conclusion

An argon discharge plasma was produced and confined by a cusped magnetic field configuration. Increase of magnetic field reduced the cusp leak width. The reduction was as good as 63.89% at the highest magnetic field to that at lowest field ($B = 40$ to 160 G) studied at the ring cusp for ions at high I_d and 70% for electrons at low I_d and at the point cusp the same was 75% ($B = 60$ to 300 G) for ions and 77.78% for electrons for $P = 5 \times 10^{-4}$ mb. The loss of plasma characterised by the leak width was found to be independent of pressure at low pressures and high magnetic fields and the leak width scaled as $B^{-1/2}$. At low pressures, high magnetic fields and high discharge currents the plasma was quasineutral. The study will be of interest for producing large volume plasmas which will be useful for basic studies and also for plasma processing.

The authors acknowledge the award of Scheme No. SP/INC/PP-21/91 by the Department of Science and Technology and one of the authors (AA) acknowledges the Senior Research Fellowship awarded by the Council of Scientific and Industrial Research, Government of India.

References

1. A. Kitsunezaki, M. Tanimoto, T. Sekiguchi, Phys. Fluids **17**, 1895 (1974).
2. N. Hershkowitz, K.N. Leung, Phys. Rev. Lett. **35**, 277 (1975).
3. K.N. Leung, N. Hershkowitz, K.R. Mackenzie, Phys. Fluids **19**, 1045 (1976).
4. M.G. Haines, Nucl. Fusion **17**, 811 (1977).
5. N. Hershkowitz, J.R. Smith, H. Kozima, Phys. Fluids **22**, 122 (1979).
6. T. Fujita, T. Ohnuma, S. Adachi, Plasma Phys. **23**, 1019 (1981).
7. H. Kozima , K. Yamagiwa, H. Itoh, K. Sakurai, Plasma Phys. **25**, 287 (1983).
8. S. Kogoshi, K.N. Sato, T. Sekiguchi, J. Phys. D **11**, 1057 (1978).
9. R.E. Pechacek, J.R. Greig, M. Raleigh, D.W. Koopman, A.W. Desilva, Phys. Rev. Lett. **45**, 256 (1980).
10. G. Knorr, D. Willis, Z. Naturforsch. **37a**, 780 (1982).
11. G. Knorr, R.L. Merlino, Plasma Phys. Controlled Fusion **26**, 433 (1984).
12. R.A. Bosch, R.L. Merlino, Phys. Fluids **29**, 1998 (1986).
13. S. Mukherjee, P.I. John, Surf. Coat. Technol. **93**, 188 (1997).
14. T. Morishita, M. Ogasawara, A. Hatayama, Rev. Sci. Instrum. **69**, 968 (1998).
15. N.A. Krall, A.W. Trivelpiece, Principles of Plasma Physics, Mc Graw Hill, New York, 1973.